

## Environmental Research Letters

---

LETTER • OPEN ACCESS

# Uncertainty in United States coastal wetland greenhouse gas inventoring

To cite this article: James R Holmquist *et al* 2018 *Environ. Res. Lett.* **13** 115005

View the [article online](#) for updates and enhancements.

### Recent citations

- [Salt marsh ecosystem restructuring enhances elevation resilience and carbon storage during accelerating relative sea-level rise](#)  
Meagan Eagle Gonneea *et al*

## Environmental Research Letters



## LETTER

## Uncertainty in United States coastal wetland greenhouse gas inventoring





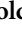











## OPEN ACCESS

RECEIVED  
5 May 2018REVISED  
28 August 2018ACCEPTED FOR PUBLICATION  
14 September 2018PUBLISHED  
12 November 2018

Original content from this work may be used under the terms of the [Creative Commons Attribution 3.0 licence](#).

Any further distribution of this work must maintain attribution to the author(s) and the title of the work, journal citation and DOI.



James R Holmquist<sup>1,14</sup> , Lisamarie Windham-Myers<sup>2</sup> , Blanca Bernal<sup>1,3</sup> , Kristin B Byrd<sup>4</sup> , Steve Crooks<sup>5</sup> , Meagan Eagle Gonneea<sup>6</sup> , Nate Herold<sup>7</sup> , Sara H Knox<sup>8</sup> , Kevin D Kroeger<sup>6</sup> , John McCombs<sup>9</sup> , J Patrick Megonigal<sup>1</sup> , Meng Lu<sup>1,13</sup> , James T Morris<sup>10</sup> , Ariana E Sutton-Grier<sup>11</sup> , Tiffany G Troxler<sup>12</sup>  and Donald E Weller<sup>1</sup> 

<sup>1</sup> Smithsonian Environmental Research Center, 647 Contees Wharf Rd, Edgewater, MD 21037, United States of America

<sup>2</sup> Water Mission Area, US Geological Survey, 345 Middlefield Road, Menlo Park, CA 94025, United States of America

<sup>3</sup> Winrock International, 2121 Crystal Drive, Arlington, VA 22202, United States of America

<sup>4</sup> Western Geographic Science Center, US Geological Survey, 345 Middlefield Road, Menlo Park, CA 94025, United States of America

<sup>5</sup> Silvestrum Climate Associates, 150 Seminary Drive, Mill Valley, CA 94941, United States of America

<sup>6</sup> Woods Hole Coastal & Marine Science Center, US Geological Survey, 384 Woods Hole Rd., Woods Hole, MA 02543, United States of America

<sup>7</sup> NOAA Office for Coastal Management, 2234 South Hobson Ave., Charleston, SC 29405-2413, United States of America

<sup>8</sup> Department of Earth System Science, Stanford University, Stanford, CA 94305, United States of America

<sup>9</sup> The Baldwin Group at NOAA Office for Coastal Management, 2234 South Hobson Ave., Charleston, SC 29405-2413, United States of America

<sup>10</sup> Belle Baruch Institute, University of South Carolina, Columbia, SC 29208, United States of America

<sup>11</sup> Earth System Science Interdisciplinary Center, University of Maryland, College Park, MD 20740 and The Nature Conservancy, Bethesda, MD 20814, United States of America

<sup>12</sup> Sea Level SOLUTIONS Center and Southeast Environmental Research Center, Institute of Water and Environment, Florida International University, Miami, FL 33139, United States of America

<sup>13</sup> School of Ecology and Environmental Science, Yunnan University, 2 North Cui Hu Road, Kunming, 650091, People's Republic of China

<sup>14</sup> Author to whom any correspondence should be addressed.

**E-mail:** [HolmquistJ@si.edu](mailto:HolmquistJ@si.edu), [lwindham-myers@usgs.gov](mailto:lwindham-myers@usgs.gov), [BernalB@si.edu](mailto:BernalB@si.edu), [kbyrd@usgs.gov](mailto:kbyrd@usgs.gov), [steve.crooks.bc@gmail.com](mailto:steve.crooks.bc@gmail.com), [mgonneea@usgs.gov](mailto:mgonneea@usgs.gov), [nate.herold@noaa.gov](mailto:nate.herold@noaa.gov), [saraknox@stanford.edu](mailto:saraknox@stanford.edu), [kkroeger@usgs.gov](mailto:kkroeger@usgs.gov), [John.McCombs@noaa.gov](mailto:John.McCombs@noaa.gov), [MegonigalP@si.edu](mailto:MegonigalP@si.edu), [LuM@si.edu](mailto:LuM@si.edu), [morris@inlet.geol.sc.edu](mailto:morris@inlet.geol.sc.edu), [a.sutton-grier@tnc.org](mailto:a.sutton-grier@tnc.org), [troxler@fiu.edu](mailto:troxler@fiu.edu) and [WellerD@si.edu](mailto:WellerD@si.edu)

**Keywords:** coastal wetland, carbon cycle, tidal wetland, saltmarsh, mangrove, tidal freshwater forest, greenhouse gas inventory

Supplementary material for this article is available [online](#)

**Abstract**

Coastal wetlands store carbon dioxide (CO<sub>2</sub>) and emit CO<sub>2</sub> and methane (CH<sub>4</sub>) making them an important part of greenhouse gas (GHG) inventoring. In the contiguous United States (CONUS), a coastal wetland inventory was recently calculated by combining maps of wetland type and change with soil, biomass, and CH<sub>4</sub> flux data from a literature review. We assess uncertainty in this developing carbon monitoring system to quantify confidence in the inventory process itself and to prioritize future research. We provide a value-added analysis by defining types and scales of uncertainty for assumptions, burial and emissions datasets, and wetland maps, simulating 10 000 iterations of a simplified version of the inventory, and performing a sensitivity analysis. Coastal wetlands were likely a source of net-CO<sub>2</sub>-equivalent (CO<sub>2</sub>e) emissions from 2006–2011. Although stable estuarine wetlands were likely a CO<sub>2</sub>e sink, this effect was counteracted by catastrophic soil losses in the Gulf Coast, and CH<sub>4</sub> emissions from tidal freshwater wetlands. The direction and magnitude of total CONUS CO<sub>2</sub>e flux were most sensitive to uncertainty in emissions and burial data, and assumptions about how to calculate the inventory. Critical data uncertainties included CH<sub>4</sub> emissions for stable freshwater wetlands and carbon burial rates for all coastal wetlands. Critical assumptions included the average depth of soil affected by erosion events, the method used to convert CH<sub>4</sub> fluxes to CO<sub>2</sub>e, and the fraction of carbon lost to the atmosphere following an erosion event. The inventory was relatively insensitive to mapping uncertainties. Future versions could be improved by collecting additional data, especially the depth affected by loss events, and by better mapping salinity and inundation gradients relevant to key GHG fluxes.

**Social Media Abstract:** US coastal wetlands were a recent and uncertain source of greenhouse gasses because of CH<sub>4</sub> and erosion.

## 1. Introduction

Managing land to optimize carbon storage and mitigate degradation is one among many strategies under consideration to curb anthropogenic greenhouse gas emissions (Griscom *et al* 2017). Coastal wetlands—defined here as salt marshes, mangroves, tidal freshwater wetlands, and tidal freshwater forests—have received some of this attention because they can act as a net-greenhouse gas sink (Howard *et al* 2017), and because restoration (Kroeger *et al* 2017) and conservation (DeLaune and White 2012) may reduce or mitigate emissions. Regulation and market mechanisms can incentivize wetland restoration to promote emission reduction (Pendleton *et al* 2012, Wylie *et al* 2016) and myriad co-benefits (Barbier *et al* 2011, Doughty *et al* 2017, Griscom *et al* 2017).

Coastal wetlands can bury carbon (Chmura *et al* 2003, Ouyang and Lee 2013, Howard *et al* 2017) and form new soil (Morris *et al* 2002) by adding organic carbon to the soil column through sub-surface root addition (Nyman *et al* 2006). Carbon burial is a dynamic response to sea-level rise (Kirwan and Megonigal 2013, Kirwan *et al* 2016). Carbon removed from the atmosphere and incorporated into soils and plant matter is referred to throughout this paper as a ‘removal’. However, wetlands can also be the sources of emissions when they are eroded (DeLaune and White 2012), developed (Stein *et al* 2014), or drained for agriculture (Drexler *et al* 2009). Freshwater and brackish tidal wetlands emit methane (CH<sub>4</sub>) (Bridgman *et al* 2006, Poffenbarger *et al* 2011), a more potent greenhouse gas than carbon dioxide (CO<sub>2</sub>) over the course of its atmospheric lifetime (Frolking and Roulet 2006, Neubauer and Megonigal 2015). At a national scale, in order to estimate total greenhouse gas emissions or removals, researchers need to know the areal coverage of different wetland types, the areal coverage of wetland change events, and to assign annualized CO<sub>2</sub> equivalent (CO<sub>2</sub>e) stock changes to those wetland classes and change events.

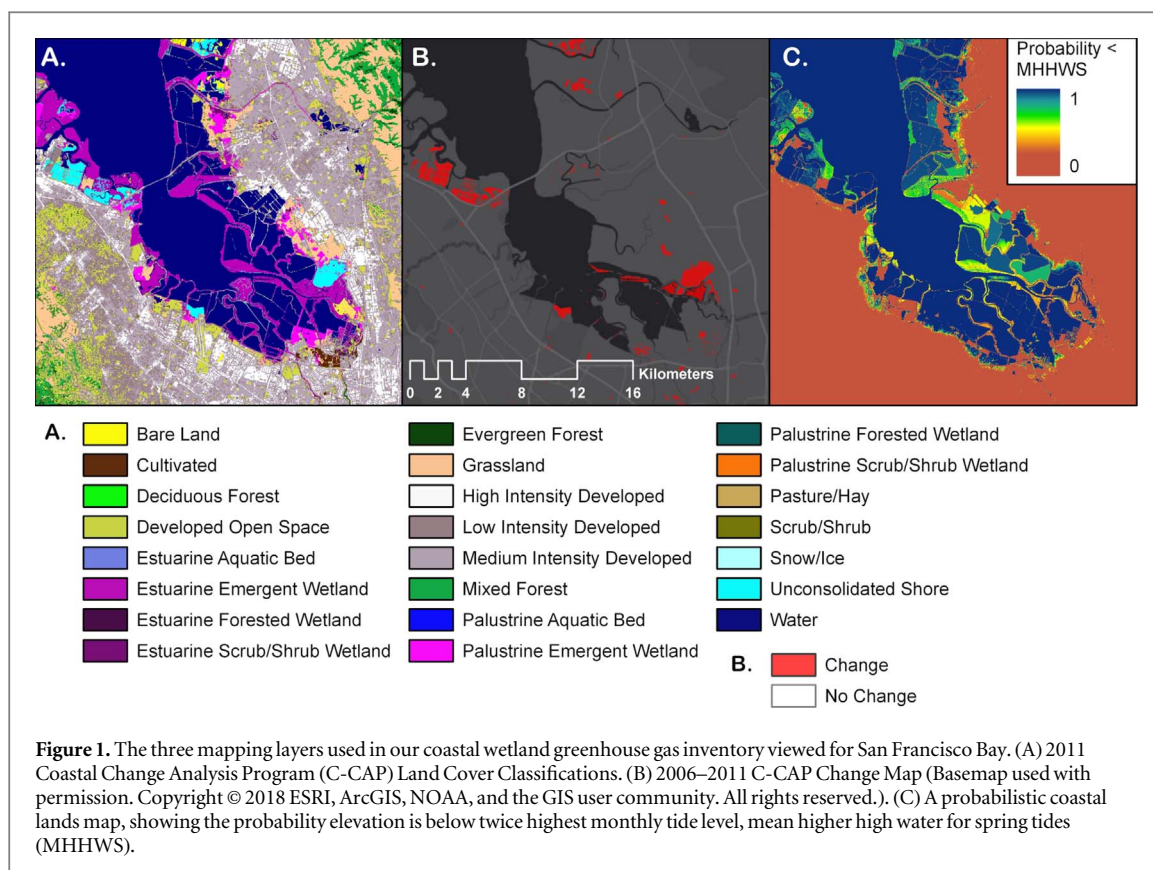
Spatial data, literature review, and expert assumptions are all used to inventory greenhouse gas fluxes at national scales. These inputs introduce uncertainty (IPCC 2014), which needs to be quantified to establish both levels of confidence and priorities for future research. The Intergovernmental Panel on Climate Change (IPCC) quantifies emissions and removals with ‘emissions factors’ and ‘activities data’. For agricultural, forested and other lands, emissions factors are values assigning greenhouse gas fluxes to land cover types and change events (equation (1)). Activities data are typically interpreted as the areal coverage of land cover type and/or land cover change events.

The IPCC published guidance for national-scale greenhouse gas inventories for coastal wetlands (IPCC 2014), and the United States incorporated these for the first time in its 2017 national greenhouse gas inventory (NGGI) conducted by the Environmental Protection Agency (EPA) (EPA 2017). Our analysis is not an official part of that NGGI. Instead, we used the accounting concepts outlined therein, as well as updated literature review and spatial data, in order to improve uncertainty estimates at the national scale and highlight areas of research that could further reduce that uncertainty.

$$\begin{aligned} \text{Emissions or Removals (flux)} &= \text{Activities (area)} \\ &\times \text{Emissions.Factor (flux / area)}. \end{aligned} \quad (1)$$

In the NGGI, uncertainties in emissions and removals were estimated using a basic algebraic approach (IPCC 2014, EPA 2017). We address five assumptions and approaches from the previous NGGI to improve uncertainty estimates in coastal wetlands: 1. The probability distributions of the activities and emissions data were not explicitly defined; 2. Key variables such as the uncertainty inherent in tidal-elevation maps were not included; 3. Uncertainties in many activities data and emissions factors are best described by non-normal distributions, which could not be accommodated using the basic algebraic approach; 4. Key assumptions, such as the depth affected by degradation events, were based on expert assessment and therefore treated as fixed values, not as probability distributions; and 5. Some inventory decisions, such as how to calculate the global warming potential (GWP) of CH<sub>4</sub> emissions and how much area to include in the inventory, have more than one recognized technique, and uncertainty from choosing among techniques was not quantified.

Our analysis expands upon the scope of the NGGI uncertainty analysis and explicitly identifies and quantifies uncertainty for key activities data and emissions factors. We update key datasets with new synthesis efforts (Windham-Myers and Cai in Revision) (supplemental information is available online at [stacks.iop.org/ERL/13/115005/mmedia](https://stacks.iop.org/ERL/13/115005/mmedia)) and the results of NASA Carbon Monitoring Systems projects (Olofsson *et al* 2014, Byrd *et al* 2018, Holmquist *et al* 2018). Our research questions are: 1. How much certainty is there that CONUS coastal wetlands were a net-source or sink of GHGs from 2006–2011? 2. Which datasets, assumptions, or mapping categories introduce the most uncertainty into the coastal wetland category of the US national GHG inventory?



## 2. Methods

We addressed our research questions by integrating multiple spatial and non-spatial datasets, explicitly defining uncertainty in each step, estimating total propagated uncertainty using a Monte Carlo analysis (Ogle *et al* 2003, IPCC 2006), and by quantifying the sensitivity of total emissions and removals to each input.

### 2.1. Time period and 2006–2011 land cover classes analyzed

As in the NGGI (EPA 2017) we quantified area using the Coastal Change Analysis Program (C-CAP; figure 1; supplemental table 1). C-CAP is a Landsat-based land cover mapping product with 23 land cover classes, including six types of intertidal wetlands defined by two types of salinity (palustrine and estuarine) and three types of vegetation (emergent, scrub/shrub, and forested) (McCombs *et al* 2016). We did not include seagrasses in this analysis because C-CAP's 'estuarine aquatic bed' category typically represents nearshore vegetated environments, such as kelp beds, which are not a net-carbon storing system (Howard *et al* 2017). The coastal wetland section of the NGGI inventory also did not include palustrine forested wetlands, since they fall under the purview of forested lands. We include them because information on their contribution to uncertainty is informative regardless of their reporting subcategory.

The NGGI inventory is required to report from 1990–2015, so they linearly interpolate C-CAP changes back to 1990 and forward to 2015 (EPA 2017). Although C-CAP produces land cover change maps for five-year intervals for all US coastal states from 1996–2011, for our analysis we focus on the C-CAP 2006–2011 time step because it is currently the only version with accuracy assessment data. From 2006–2011 we mapped 240 different land cover types including, six classes of wetlands that had the same classification in 2006 and 2011, and 234 types of change to, from, and between wetland classes.

### 2.2. Overview of inventory calculations

We quantified total US GHG emissions and removals from coastal wetlands by mapping the area of different classes of stable wetlands and different types of change events, then multiplying that area by the summed soil, biomass and methane flux from 2006–2011 (equation (2))

$$\text{total.flux} = \sum_{(i=1)}^n \text{estimated.area}_i (\text{soil.flux}_i + \text{biomass.flux}_i + \text{methane.flux}_i). \quad (2)$$

In which:

$i$  is a 2006–2011 land cover class in  $n$  land cover classes

$\text{estimated area}_i$  is the total area of land cover class  $i$

Each flux is the mass CO<sub>2</sub>e emitted or stored per unit area for land cover class  $i$ .

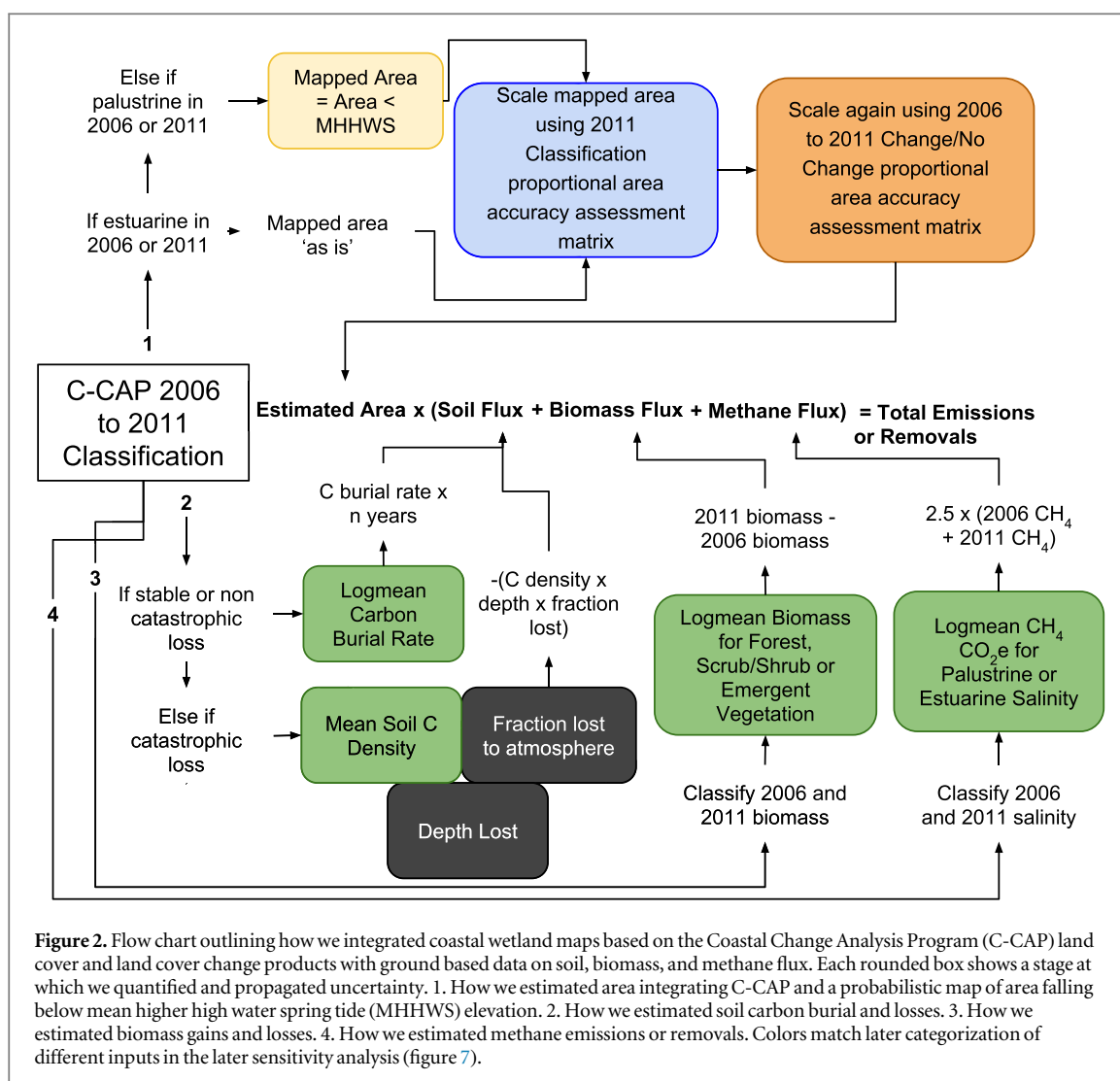


**Figure 2.** Flow chart outlining how we integrated coastal wetland maps based on the Coastal Change Analysis Program (C-CAP) land cover and land cover change products with ground based data on soil, biomass, and methane flux. Each rounded box shows a stage at which we quantified and propagated uncertainty. 1. How we estimated area integrating C-CAP and a probabilistic map of area falling below mean higher high water spring tide (MHHWS) elevation. 2. How we estimated soil carbon burial and losses. 3. How we estimated biomass gains and losses. 4. How we estimated methane emissions or removals. Colors match later categorization of different inputs in the later sensitivity analysis (figure 7).

As in the US coastal NGGI, we defined the area of interest as the CONUS and included all C-CAP estuarine wetlands (figure 2) and palustrine wetlands occurring at an elevation below the highest tides. This is referred to throughout as the coastal lands definition. Since estuarine wetlands as C-CAP defines them are driven by oceanic tidal influence, we used mapped area as represented in C-CAP as fixed values (figure 2). Since palustrine wetlands can either be tidal or non-tidal, we used a probabilistic map of areas falling below mean higher high water spring (MHHWS) tides to map palustrine wetland area falling within the coastal zone. Palustrine wetland mapped areas were not treated as fixed values; we estimated them as a probability distribution using a mean ( $\mu_{pal,i}$ ) and standard deviation ( $\sigma_{pal,i}$ ) for each class ( $i$ ), derived from the probabilistic MHHWS map (equation (3))

$$\text{mapped.area}_{pal,i} \sim \text{normal}(\mu_{pal,i}, \sigma_{pal,i}). \quad (3)$$

Our analysis made a distinction between mapped area and estimated area. Estimated area can be greater than or less than mapped area because unequal omission errors (errors of exclusion) and commission error (errors of inclusion) can cause a land cover class to be

over- or under-mapped. We scaled mapped area by taking into account potential errors in 2011 classification (Olofsson *et al* 2014) as well as 2006–2011 change detection (figure 2). In a simplified version of this concept, accuracy assessment matrices containing counts of true classifications and misclassifications, can be simplified down to a single estimated-to-mapped area ratio ( $r$ ) for a classification ( $i$ ) (equation (4)). This value will be less than one if a land cover class is over-mapped, and greater than 1 if a land cover class is under-mapped

$$\text{estimated.area}_i = r_i \times \text{mapped.area}_i. \quad (4)$$

We estimated total emissions or removals by multiplying estimated area by the summed per area flux of soil and biomass  $\text{CO}_2$  and  $\text{CH}_4$   $\text{CO}_2\text{e}$  (figure 2). For emissions factors we treated flux data as it was reported (either positive or negative), but transformed them when necessary, so that any emissions were always represented as a negative value and removals were always represented as a positive value. For soils, if the land cover type did not change or changed but did not result in soil loss (supplemental information 2.3.1), then soil carbon flux was estimated as the annual soil carbon burial rate multiplied by the number of years

that wetlands were present (equation (5)). If the 2006–2011 class changed and represented a soil loss event, such as conversion to developed, agricultural land, or open water, then emissions were estimated to be the product of mean soil carbon density, depth lost, and fraction of that returns to the atmosphere (equation (6)). We quantified biomass using three vegetation classes: forested, scrub/shrub, and emergent vegetation. We estimated biomass flux if there was a transition between vegetation types or from vegetated to unvegetated surfaces between 2006–2011 (equation (7)). We quantified CH<sub>4</sub> fluxes using two salinity classes, since freshwater wetlands (palustrine) emit more methane than brackish to saline wetlands (estuarine) (Poffenbarger *et al* 2011). We calculated methane flux for a class by determining CH<sub>4</sub> emissions associated with the salinity type in 2006 and 2011, summing them, and multiplying by 2.5 to normalize the flux over five years (equation (8))

$$\text{soil.flux}_{no.loss} = \text{soil.burial} \times n.\text{years}, \quad (5)$$

$$\text{soil.flux}_{loss} = -(\text{soil.carbon} \times \text{depth.lost} \times \text{fraction.returned}), \quad (6)$$

$$\text{biomass.flux} = \text{biomass}_{2011} - \text{biomass}_{2006}, \quad (7)$$

$$\text{methane.flux} = -2.5 (\text{methane}_{2011} + \text{methane}_{2006}). \quad (8)$$

### 2.3. Estimating area of wetland class and change events

#### 2.3.1. Using tide and elevation data to map coastal palustrine wetlands

As in the previous NGGI, we mapped a subset of palustrine wetlands categorized as coastal lands because their tidal elevation was lower than MHHWS. However, uncertainties in digital elevation model (DEM) elevations and in mapping tidal height were not previously included in the NGGI uncertainty analysis (EPA 2017). We enhanced the inventory by creating a probabilistic coastal lands map (supplemental information: section 2.1).

For wetland surface elevation data we used DEMs that were created using Light Detection and Ranging (LiDAR) and were aggregated by the National Oceanic and Atmospheric Association (NOAA) for their Sea-Level Rise Viewer (supplemental table 1). DEMs were created to Federal Emergency Management Administration accuracy standards (ASPRS 2004, Covey 2013). DEMs have a nominal root mean square error (RMSE) of 0.185 m for low-relief areas and assume no bias (supplemental table 1). However, wetland vegetation and soil introduce system-specific bias and random error (Chassereau *et al* 2011) not captured by the nominal accuracy reporting. We corrected for a mean error of 0.173 m and estimate a RMSE of 0.205 m for wetland surfaces based on a weighted average of results from multiple US-based studies (supplemental table 2). We created a map of MHHWS heights using empirical Bayesian kriging to interpolate between NOAA tide gauges. We also

created a corresponding uncertainty map incorporating random error in LiDAR mapping, datum transformations (Schmid *et al* 2013, Leon *et al* 2014), and distance between tide gauges. We combined the DEMs, the MHHWS map, and the associated uncertainty surfaces into a single spatial layer representing the probability of elevation being below MHHWS (figures 1, 2).

For palustrine wetlands, we treated mapped area as a random variable. For each of 111 palustrine wetland categories we extracted pixel counts by probability class for the coastal lands map intersecting the C-CAP class and represented mapped area as a normal distribution approximated from the multiple binomial distributions (supplemental information: section 2.1). The means and standard deviations for all 111 palustrine wetland stable classes and palustrine wetland change events are reported in supplemental table 2.

#### 2.3.2. Representing uncertainty in land cover classification and change detection

We calculated an estimated area from mapped area (Olofsson *et al* 2014, Byrd *et al* 2018) by combining accuracy assessment matrices (McCombs *et al* 2016) with area data from C-CAP (supplemental table 1) (supplemental tables 4–5). C-CAP did not assess classification accuracy for all individual land cover change events between 2006–2011. Instead there is an overall accuracy assessment for 2011 classification and one for the 2006–2011 generalized ‘change’ or ‘no change’ categories.

The accuracy assessment matrix records counts for all instances of mapped classes—what a datapoint was mapped as—and reference classes—what it actually was (supplemental tables 4–5). We converted the accuracy assessment matrix from counts to proportional areas (Olofsson *et al* 2014, Byrd *et al* 2018), and calculated the estimated proportional area for each class as the reference class’ column sum in the proportional area matrix. We used estimated and mapped area at the full map scale to calculate an estimated to mapped area ratio ( $r$ ). For each 2006–2011 C-CAP class, we used the appropriate  $r$  to scale mapped area by the 2011 class. We then used a second  $r$  value from the ‘change’ and ‘no change’ matrix to scale again based on change detection. Additional detail on how we calculated proportional area accuracy assessment matrices and class-specific scaling factors are available in the supplemental information: section 2.2).

We represented uncertainty in estimated to mapped area ratio by representing each mapped class in the accuracy assessment count matrix as a multiple multinomial distributions, a distribution that describes counts falling into two or more categories as a random variable (supplemental information: section 2.2).

## 2.4. Carbon storage and emissions data

As in the NNGI we calculated emissions factors for soils, and CH<sub>4</sub> based on literature review and synthesis. Unlike the NNGI we include carbon fluxes related to biomass because data is now available as part of a remote sensing calibration and validation effort (Byrd *et al* 2018), and a literature review that is part of continued inventory development (supplemental information: section 2.3). We did not include N<sub>2</sub>O emissions.

### 2.4.1. Soil flux data

We estimated soil carbon stock change in wetlands remaining wetlands and lands converted to wetlands as annual carbon burial rate from a literature review of lead-210 (<sup>210</sup>Pb) dated cores (supplemental information; section 2.3.1). <sup>210</sup>Pb-based measurements typically integrate carbon burial over a century, compared to cesium-137 (<sup>137</sup>Cs)- and artificial plot-based measurements, which integrate carbon burial over multi-decadal to annual time scales; therefore we assumed <sup>210</sup>Pb-based rates are more representative of long-term storage rates. We described soil carbon burial using a lognormal distribution because observed removals can not be negative when strictly relying on dated sediment profiles, observed values were always greater than zero, and the data show a positively skewed distribution (figure 3; table 1).

For soil carbon stock change associated with wetland loss, we used average soil carbon density values reported by Holmquist *et al* (2018) to characterize the CO<sub>2</sub> emission rate (table 1). Holmquist *et al* (2018) determined that soil carbon density did not vary significantly by depth, and that the probability distribution of soil carbon density was described well by a normal distribution, truncated so that values could not be less than zero. They also determined utilizing a single average value for all wetlands was more parsimonious and precise than stock estimates based on available maps of soil carbon.

The previous NNGI (EPA 2017) made two assumptions about carbon changes during wetland conversion events that were not considered in the error propagation. First, the depth of soil lost to conversion was based on a range of values reported for aquaculture and salt production pond construction (0.5–2.5 m; IPCC 2014) but was fixed to 1 m. In the NNGI, this value was applied to wetland areas that converted to open water as indicated by C-CAP. Because wetland to open water conversion events were dominant in our accounting and the IPCC depth intervals for degradation were largely not applicable, we represented uncertainty regarding this assumption by using a uniform distribution ranging from 0.5–1.5 m (table 1) to represent a wide distribution centered on 1 m. This uncertainty reflected a consensus from our coauthor group and reflected an expert assumption rather than data, as we could not readily locate or ingest any relevant data. The NNGI also assumed that

100% of the carbon released by conversion from coastal wetlands to open water is lost to the atmosphere. However (Lovelock *et al* 2017) reviewed available studies and estimated 25%–50% of terrestrial carbon delivered to the marine environment was buried in ocean sediments (Baldock *et al* 2004, Cai 2011, Blair and Aller 2012). Therefore we represented the fraction lost back to the atmosphere as a uniform distribution ranging from 50%–75% (table 1).

### 2.4.2. Biomass flux data

We utilized biomass data from (Byrd *et al* 2018) to generate emissions factors for emergent wetlands. We accounted for forested wetland biomass using a synthesis of tree diameter at breast height (DBH) for mangrove and tidal freshwater forested plots, then converting DBH to above ground biomass using allometric equations cited within the data source, or originating from a similar representative study (supplemental information: section 2.3.2). We represented scrub/shrub data using a subset of the Byrd *et al* (2018) biomass data, plots that were dominated by the shrub *Iva frutescens*, and a subset of the forested biomass dataset, plots in which average tree heights were lower than 5 m. We converted biomass to organic carbon using a conversion factor of 0.441 (Byrd *et al* 2018). We represented above-ground biomass with lognormal distributions because the data exhibited skewed positive distributions (table 1; supplemental figure 2).

### 2.4.3. Methane flux data

For CH<sub>4</sub> fluxes, we utilized a synthesis of annual CH<sub>4</sub> fluxes compiled by (Poffenbarger *et al* 2011) and further developed as part of the 2nd State of the Carbon Cycle Report (Windham-Myers and Cai in Revision) (supplemental information: section 2.3.3). Although IPCC guidance recommends separating CH<sub>4</sub> emissions by salinity class using an 18 ppt threshold (IPCC 2014), C-CAP's two salinity categories are not optimized for this purpose. We instead had to represent CH<sub>4</sub> emissions with separate estuarine and palustrine emissions factors based on a 5 ppt salinity threshold (Dobson *et al* 1995) (figure 4).

We represented CH<sub>4</sub> fluxes using a normal distribution for estuarine wetlands because while the vast majority of sites indicated a net emissions scenario, one oligohaline site in New Jersey displayed net-uptake of CH<sub>4</sub> for much of the two years reported (Weston *et al* 2014) (figure 3). We represented palustrine CH<sub>4</sub> emissions using a lognormal distribution because flux values had a skewed positive distribution and there were no instances of net-uptake of CH<sub>4</sub> (figure 3; table 1). We estimated the GWP of CH<sub>4</sub> as 25 CO<sub>2</sub>e CH<sub>4</sub><sup>-1</sup> for consistency with the NNGI (IPCC 1997, EPA 2017) even though IPCC 5th Assessment Report recommends updated conversions (28 CO<sub>2</sub>e CH<sub>4</sub><sup>-1</sup> or 34 CO<sub>2</sub>e CH<sub>4</sub><sup>-1</sup> with feedbacks; table 1) (Pachauri *et al* 2014).

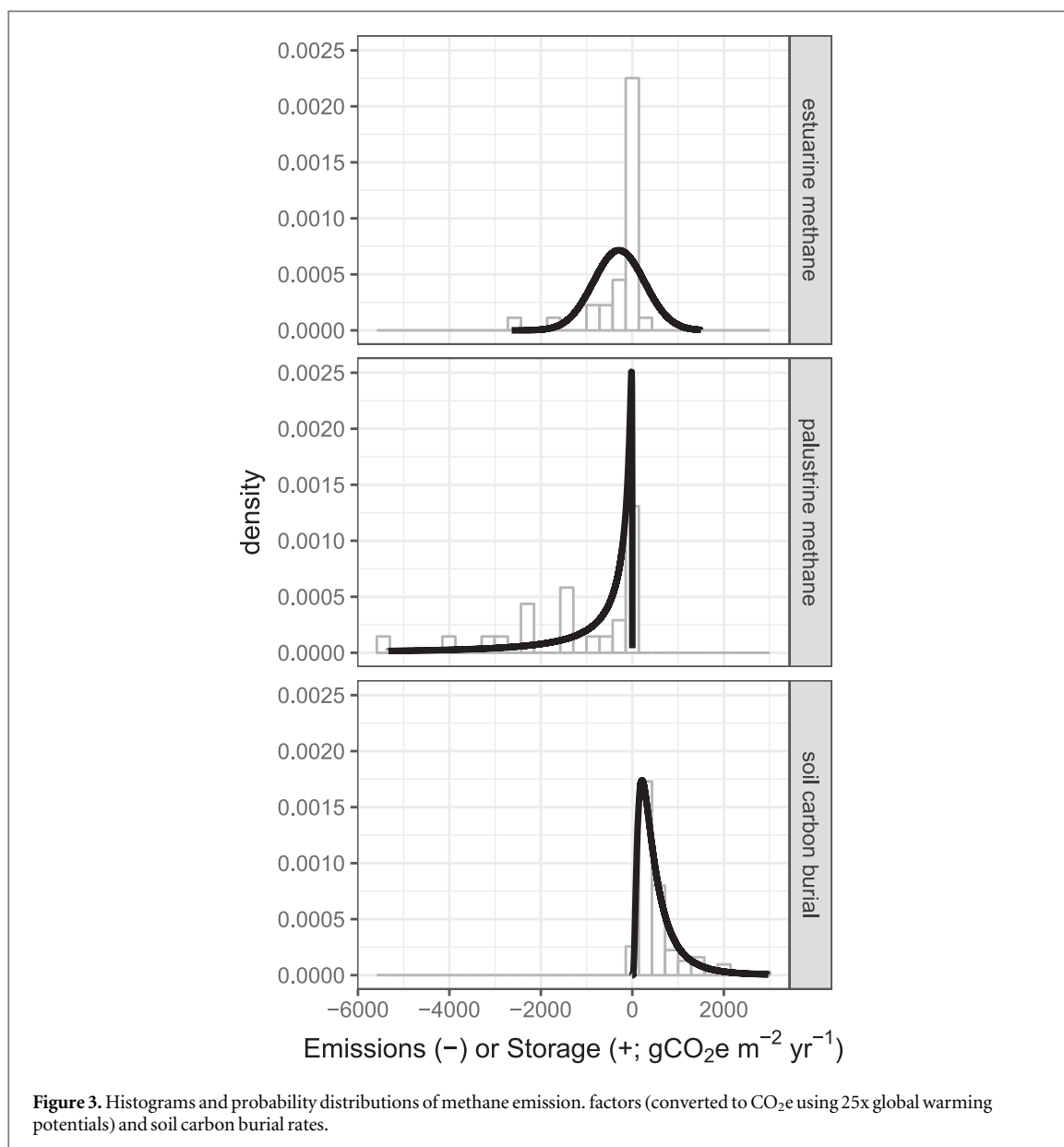


**Figure 3.** Histograms and probability distributions of methane emission factors (converted to CO<sub>2</sub>e using 25x global warming potentials) and soil carbon burial rates.

**Table 1.** Summary of probability distributions and dataset sizes used to simulate emissions factors in the Monte Carlo analysis:  $\mu$  = mean,  $\sigma$  = standard deviation,  $\alpha$  = mean of the natural log-transformed data,  $\beta$  = standard deviation of the natural log-transformed data, and min and max are the minimum and maximum values of a uniform distribution.

Emissions factor or emission factor component	Probability distribution	$n$	Moment 1	Moment 2
Carbon Burial (gCO <sub>2</sub> m <sup>-2</sup> yr <sup>-1</sup> )	Lognormal	109	$\alpha = 5.98$	$\beta = 1.05$
Soil carbon density (gCO <sub>2</sub> m <sup>-3</sup> )	Truncated normal	8280	$\mu = 99000$	$\sigma = 47667$
Depth of soil affected by loss events (m)	Uniform	1	Min = 0.5	Max = 1.5
Soil carbon fraction returned to atmosphere (fraction)	Uniform	1	Min = 0.5	Max = 0.75
Emergent biomass change (gCO <sub>2</sub> m <sup>-2</sup> )	Lognormal	2345	$\alpha = 6.36$	$\beta = 1.04$
Scrub/shrub biomass change (gCO <sub>2</sub> m <sup>-2</sup> )	Lognormal	33	$\alpha = 8.21$	$\beta = 1.97$
Forested biomass change (gCO <sub>2</sub> m <sup>-2</sup> )	Lognormal	79	$\alpha = 10.57$	$\beta = 0.75$
Estuarine CH <sub>4</sub> emissions (GWP; gCO <sub>2</sub> e m <sup>-2</sup> yr <sup>-1</sup> )	Normal	31	$\mu = 292.10$	$\sigma = 558.21$
Palustrine CH <sub>4</sub> emissions (GWP; gCO <sub>2</sub> e m <sup>-2</sup> yr <sup>-1</sup> )	Lognormal	24	$\alpha = 6.10$	$\beta = 1.80$
Estuarine CH <sub>4</sub> emissions (SGWP/SGCP; gCO <sub>2</sub> e m <sup>-2</sup> yr <sup>-1</sup> )	Normal	31	$\mu = 477.87$	$\sigma = 1061.80$
Palustrine CH <sub>4</sub> emissions (SGWP/SGCP; gCO <sub>2</sub> e m <sup>-2</sup> yr <sup>-1</sup> )	Lognormal	24	$\alpha = 6.69$	$\beta = 1.80$

## 2.5. Uncertainty and sensitivity analysis

### 2.5.1. Monte carlo analysis

We propagated uncertainty using a Monte Carlo analysis (Ogle *et al* 2003, IPCC 2006, Metsaranta

*et al* 2017). We calculated the inventory (equation (2)) 10 000 times, simulating the underlying data using random draws from the probability distributions for 145 random variables (supplemental information:



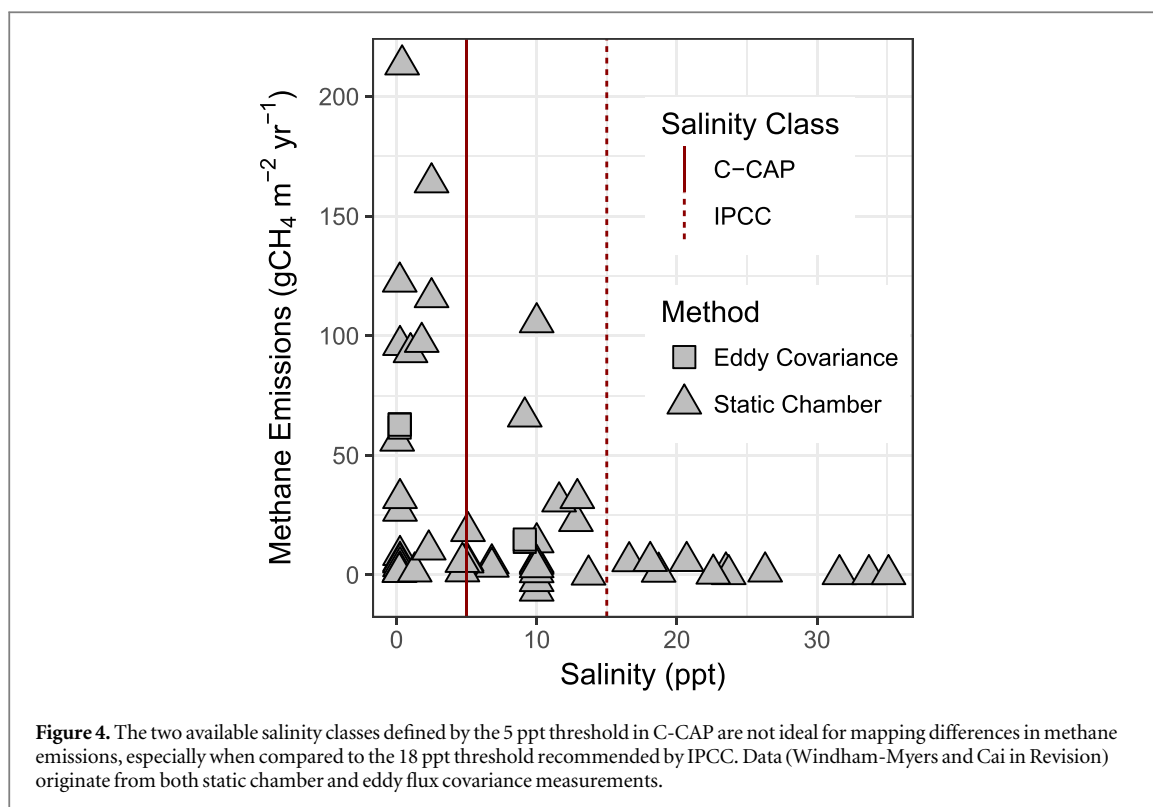


**Table 2.** Medians and confidence intervals for CONUS coastal wetland emissions (–) and storage (+) from 2006–2011 in million tonnes (Teragrams) of CO<sub>2</sub>-equivalent (CO<sub>2</sub>e) per year.

Land cover change type analyzed	Lower confidence interval (0.025)	Median (0.5)	Upper confidence interval (0.975)
Estuarine losses	–13.3	–8.1	–4.1
Estuarine stable and gains	–2.3	2.2	6.7
Palustrine losses	–3.7	–2.4	–1.3
Palustrine stable and gains	–9.6	–1.5	2
Total	–21.3	–10.3	–1.3

section 2.3.4): including normal distributions for the mapped area for each of 111 possible palustrine stable and change classes (supplemental table 2) and multinomial distributions used to randomly draw accuracy assessment matrices for twenty-three 2011 C-CAP land cover classifications (supplemental table 4), and 2006–2011 change and no change categories (supplemental table 5).

We also propagated uncertainty for nine emissions factors or emission factor components (table 2). For normally distributed variables we randomly drew the same number of datapoints from literature review from the probability distribution then represented the emissions factor or component as the mean of the randomly drawn data. For uniform distributions, we randomly drew a single value. For emissions factors that were lognormally distributed we randomly redrew the underlying data as in normal distributions but represented the central tendency of using the exponentiated logmean. This choice is consistent with IPCC *Wetlands Supplement* guidance, however arithmetic means are often used for lognormally distributed emissions factors (Levy *et al* 2017). Because the goal of this paper

is to quantify the effect of assumptions on the inventory, we repeated the uncertainty analysis using the arithmetic mean of lognormally distributed values (supplemental information: section 3.2; supplemental figure 4).

#### 2.5.2. Sensitivity analysis

We performed a one-at-a-time sensitivity analysis (Metsaranta *et al* 2017), meaning we categorized sensitivity of the US scale emissions and removals to assumptions, datasets, and mapping accuracies by manipulating one input at a time and recording the effect. For each random variable we re-calculated the coastal wetland total GHG emissions and removals using the 0.025 quantile and 0.975 quantile values from Monte Carlo analysis, while fixing all others at their median value. We reported sensitivity of the inventory to each input as the difference in the total flux between using the input's minimal and maximal settings.

The sensitivity analysis also helped test the effect of some of the fundamental assumptions. For example, CH<sub>4</sub> fluxes need to be converted to CO<sub>2</sub>e, and there is

controversy about whether to use the GWP (25 CO<sub>2</sub>e CH<sub>4</sub><sup>-1</sup>) (IPCC 2014) or the Sustained Global Warming Potential (SGWP; 45 CO<sub>2</sub>e CH<sub>4</sub><sup>-1</sup>) and Sustained Global Cooling Potentials (SGCP; 203 CO<sub>2</sub>e g CH<sub>4</sub><sup>-1</sup>) which more effectively represent the system (Neubauer and Megonigal 2015). We quantified the effect of that choice by calculating the inventory using a GWP and median values for all other inputs and then recalculated changing only the GWP to SGW/CP (Neubauer and Megonigal 2015). Also, we tested the assumption of relying on the coastal lands definition for determining how much palustrine wetland area to include in the inventory compared to a tidal wetlands definition from the National Wetlands Inventory (NWI) (Hinson *et al* 2017, Holmquist *et al* 2018, Najjar *et al* 2018). For this alternative analysis, we included all C-CAP palustrine wetlands intersecting an NWI-based tidal wetlands map (Holmquist *et al* 2018) and treated all palustrine mapped areas as fixed. In the sensitivity analysis we calculated the difference in total inventory between the default settings and the NWI based mapping strategy. We also we repeated the sensitivity analysis using the arithmetic mean of lognormally distributed values, and discuss the results further in the supplemental information (section 3.2; supplemental figure 5).

### 3. Results and discussion

#### 3.1. Initial assessment of estimated area

The Monte Carlo analysis combining C-CAP and LiDAR DEMs define a total area of interest with a median of 3.56 million hectares (M ha; figure 5). Stable wetlands were the largest category (figure 5) with estuarine emergent wetlands dominating (1.82 M ha), followed by palustrine forested wetlands (0.68 M ha), palustrine emergent wetlands (0.54 M ha), and estuarine forested wetlands (0.19 M ha). Of the wetlands that changed to or from other categories, loss of emergent wetlands to open water was the most dominant classification. Conversion from open water to emergent wetlands was the next most important conversion but only made up for one third of the area converted from emergent wetlands to open water. The NWI-based strategy mapped fewer palustrine wetlands, especially palustrine forested wetlands, defining a total area of interest of 2.86 M ha.

#### 3.2. Uncertainty in the CONUS 2006–2011 coastal wetland inventory

Coastal wetlands were likely to have acted as a net-source of GHG from 2006 to 2011 (figure 6; table 1; supplemental table 7). Across the 10 000 Monte Carlo iterations median total net-emission was -10.3 million tonnes (M tonnes) of CO<sub>2</sub>e per year (yr<sup>-1</sup>) over five years with a confidence interval ranging from -1.6 to -21.3 M tonnes CO<sub>2</sub>e yr<sup>-1</sup>. Although the confidence intervals were wide they were strictly

negative, which support the conclusion of net-emissions from 2006–2011.

Separating estuarine wetlands, which have lower CH<sub>4</sub> emissions, and palustrine wetlands, which have higher CH<sub>4</sub> emissions, indicates that both classes are more likely to have acted as net-emitters (table 2). However, estuarine wetlands emissions were more likely occurring due to wetland conversion events (figure 6). While overall stable and gaining estuarine wetlands acted as a net-sink and stable and gaining palustrine wetlands a net-source according to their median values, both categories had uncertainties spanning both net-emissions and net-storage scenarios.

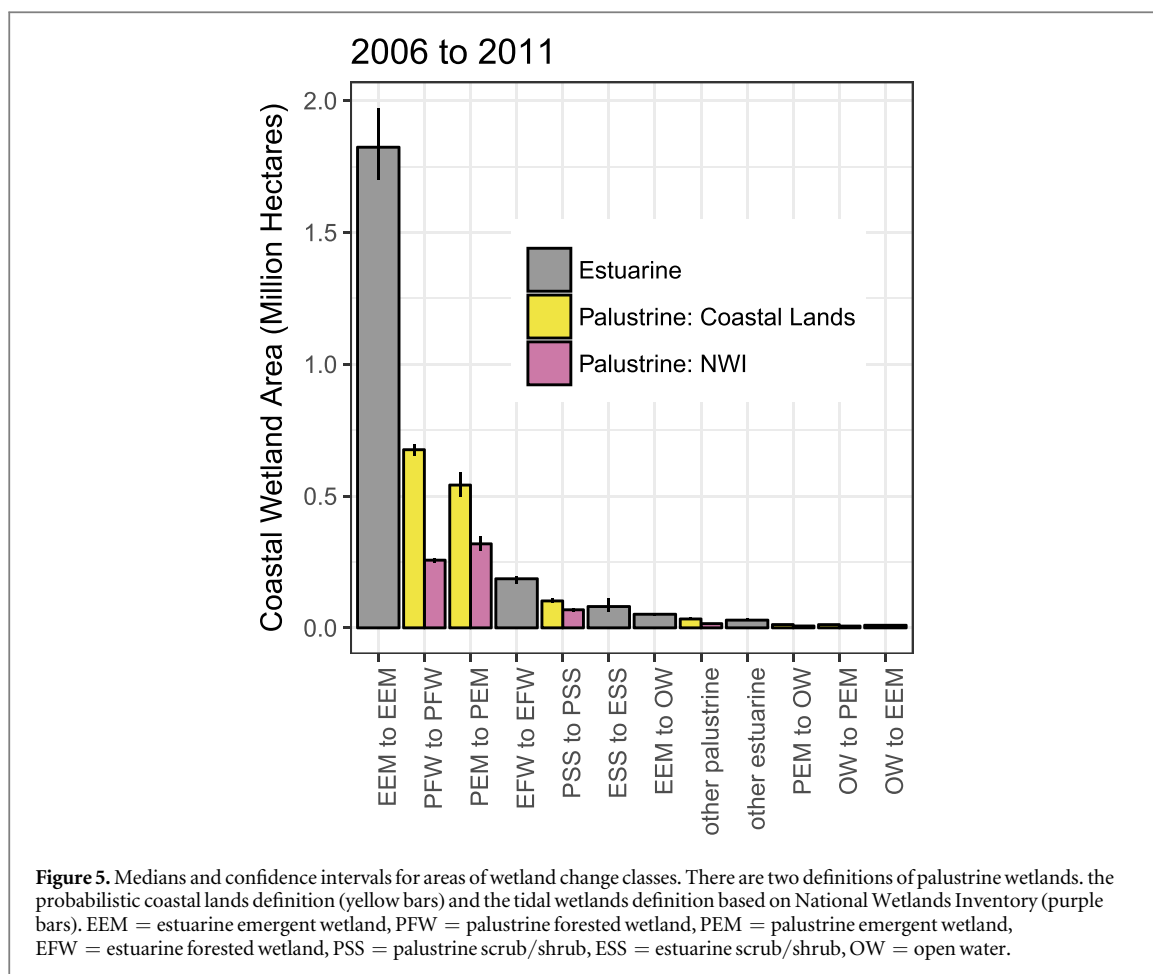
#### 3.3. The dominant contributions to national-scale uncertainty

CONUS-scale total flux was most sensitive to inputs in four major classes: uncertainty in emissions and burial data, assumptions about how to calculate the inventory, C-CAP 2006–2011 change detection accuracy, and C-CAP 2011 classification accuracy (figure 7; supplemental table 7). Overall the inventory was most sensitive to uncertainty in the underlying emissions and storage data, and to assumptions made. Uncertainty arising from the probabilistic coastal lands mapping was not a dominant contributor to total uncertainty in this framework.

Uncertainty in palustrine CH<sub>4</sub> emissions, had the greatest effect on the inventory estimates for CONUS coastal wetlands, 11.6 M tonne CO<sub>2</sub>e yr<sup>-1</sup> (figure 7; supplemental table 7). The average depth of soils lost to erosion, extraction, or drainage, was second most impactful and had a 9.4 M tonne CO<sub>2</sub>e yr<sup>-1</sup>. Estuarine CH<sub>4</sub> emissions were also important and had a 8.5 M tonne CO<sub>2</sub>e yr<sup>-1</sup> effect. Soil carbon burial rate had a 5.2 M tonne CO<sub>2</sub>e yr<sup>-1</sup> effect and assumptions made about the fraction of soil carbon lost to the atmosphere had a 3.9 M tonne CO<sub>2</sub>e yr<sup>-1</sup> effect.

The decision to use GWP over SGWP/CP had a median effect of 8.8 M tonnes of CO<sub>2</sub>e yr<sup>-1</sup>. The alternate choice moved the estuarine stable and gains sector from net-storing (+2.2 M tonnes CO<sub>2</sub>e yr<sup>-1</sup>) using GWP to net-emitting (-2.0 M tonnes CO<sub>2</sub>e yr<sup>-1</sup>) using SGW/CP (figure 7; supplemental table 8). Emissions from stable palustrine wetlands overtook palustrine soil and biomass losses when using SGW/CP. The SGW/CP choice increased the estimate of total CO<sub>2</sub>e emissions 89% over the traditional GWP model.

Uncertainty in mapping also contributed to uncertainty in the inventory. 2006–2011 change detection was the most uncertain mapping category. Notably, we drew a different conclusion regarding the 2006–2011 change than the official C-CAP accuracy assessment (McCombs *et al* 2016). We concluded that change was under-mapped while McCombs *et al* concluded change was over-mapped (supplemental information: section 3.1; supplemental figure 3). This



occurred because McCombs *et al* raw counts for the accuracy assessment matrix and we used a proportional area matrix (Olofsson *et al* 2014).

Sensitivity of the inventory to input uncertainty dropped precipitously for the remaining inputs. These include the decision between using a coastal lands definition to identify palustrine wetlands and the stricter NWI-based definition (2.0 M tonne CO<sub>2</sub>e yr<sup>-1</sup> effect) (figure 7; supplemental table 7). The effect of uncertainty in fluxes associated with changes in forested and scrub/shrub biomass and carbon density for eroded soils range from 0.6 to 0.1 M tonnes CO<sub>2</sub>e yr<sup>-1</sup>. Classification accuracy introduced uncertainty for estuarine aquatic beds, open water, unconsolidated shore and palustrine aquatic beds. In our accounting, these all indicate soil loss events.

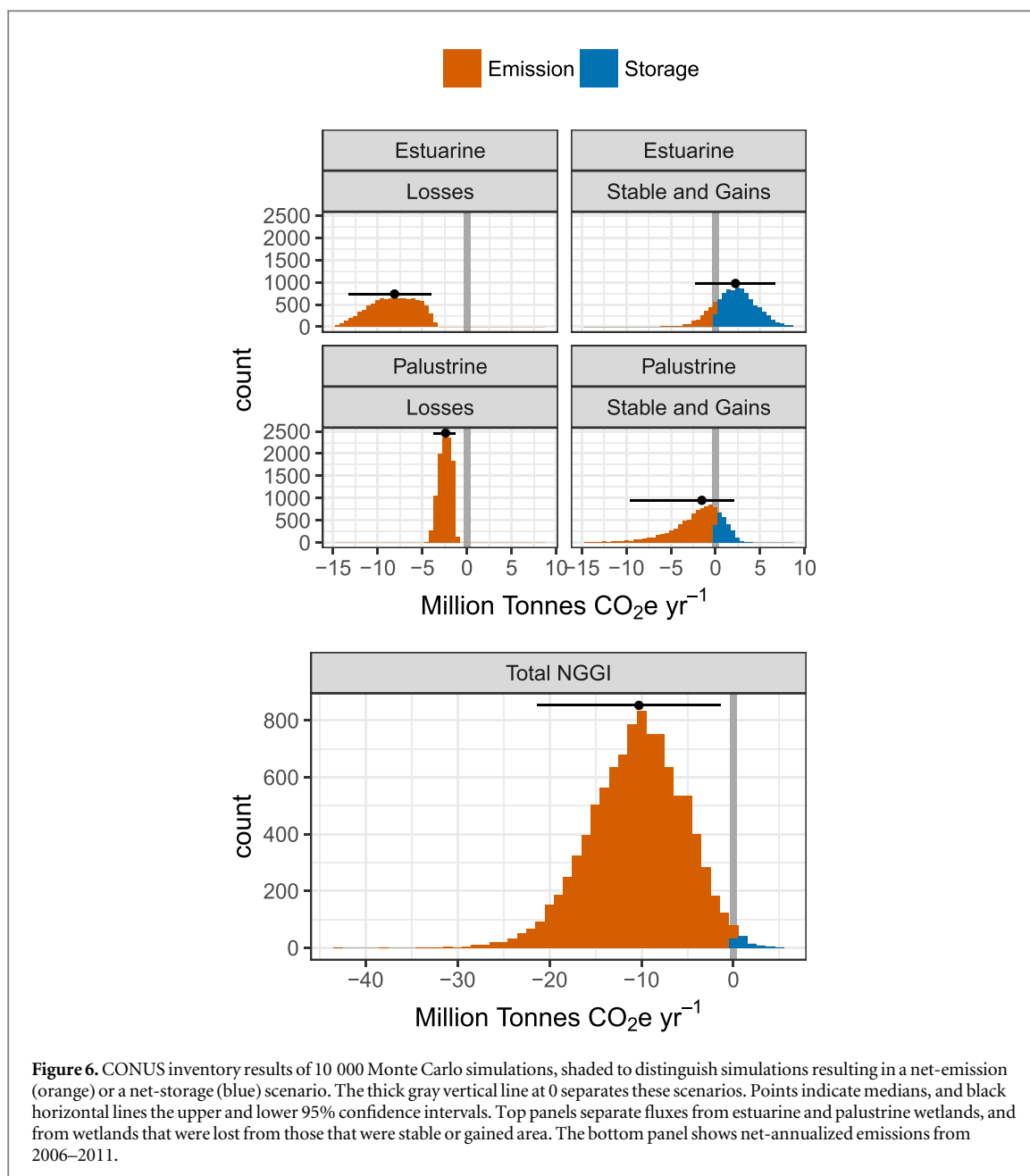
### 3.4. Implications for future research

Uncertainty estimates are important components of complete and transparent GHG inventories (EPA 2017). Uncertainty information is not intended to dispute the validity of the estimates, but rather to help prioritize efforts to improve accuracy and guide future decisions. We recommend improving process models for CH<sub>4</sub> emissions and soil carbon burial, increasing the number of observations for key inputs, and developing more detailed and accurate maps for

categories relevant to coastal wetland carbon cycling and inventory estimates.

#### 3.4.1. Improving process models for CH<sub>4</sub> emissions and soil carbon burial

The uncertainty and sensitivity analysis presented herein suggest that uncertainty could be reduced at the scale of the contiguous US primarily by improving data availability and process-based models for CH<sub>4</sub> emissions, CH<sub>4</sub> radiative forcing, and carbon burial rates. Net-wetland CH<sub>4</sub> emission combines CH<sub>4</sub> production by methanogenic archaea under anaerobic conditions, CH<sub>4</sub> oxidation and consumption by methanotrophic bacteria mainly under aerobic conditions, and CH<sub>4</sub> transport to the atmosphere (Conrad 1989, Whalen 2005). Major controls of these processes include: water table position; soil temperature; sulfate supply and potential production of hydrogen sulfide, a methanogen toxin, for which salinity is a proxy for; vegetation, including both biomass and species composition, which may facilitate CH<sub>4</sub> transport from soil production sites to the atmosphere; and primary production of vegetation, since new photosynthate may be a substrate for methanogenesis (Wang *et al* 1996, Walter and Heimann 2000). Large discrepancies have also been noted between chamber and eddy covariance measurements of CH<sub>4</sub> fluxes (Hendriks *et al* 2010,

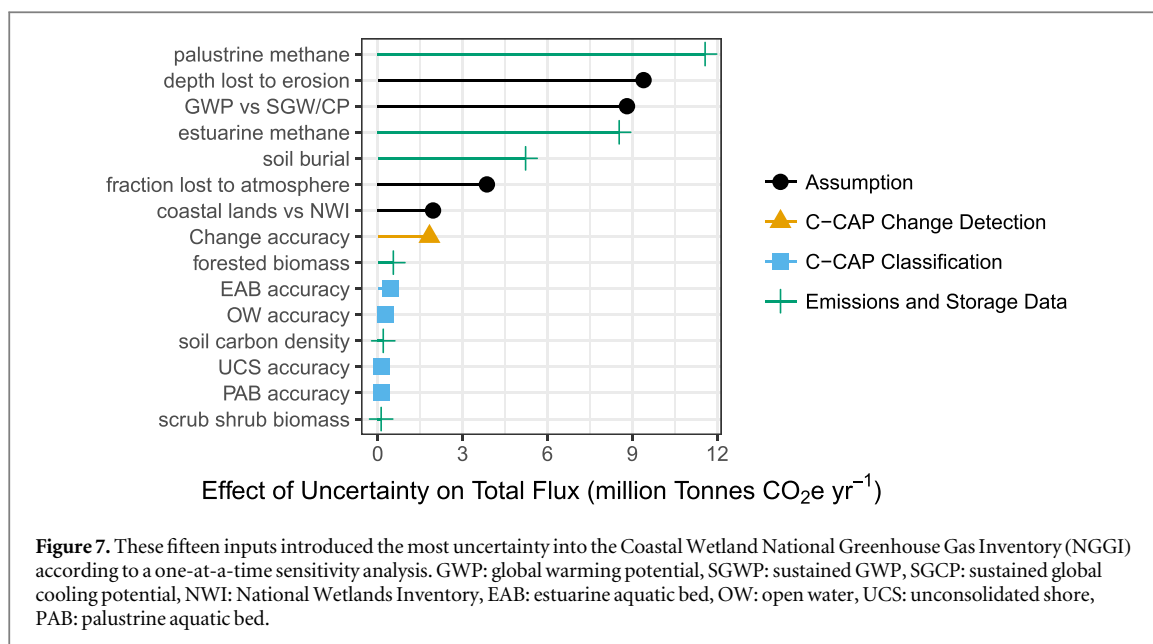


Krauss *et al* 2016), suggesting the need for additional comparisons between these two methods.

The use of GWPs serves an important policy need because GWPs are transparent and tractable. However, GWPs are an oversimplification because modeling CO<sub>2</sub>e in power units (W m<sup>-2</sup>) that relate directly to radiative forcing is several steps removed from actual climate impacts such as changes in temperature, precipitation, and sea level. The SGW/CP model is equally transparent and tractable, but more closely represents reality by acknowledging that changes in GHG emissions persist over several years (Neubauer and Megonigal 2015). Therefore we recommend that SCW/CP's should be considered for adoption by the IPCC. When considering the consequences of GHG inventory data beyond the IPCC context, ecosystem scientists and policy analysts should discuss metrics

that are independent of time frames, such as switch-over time, as they are more informative of the long-term impacts (Frolking and Roulet 2006). Our uncertainty analysis is focused on variables that are inputs to GWP and SGW/CP models, but there is an ongoing need to address the uncertainty introduced by using these models to underpin climate policy.

Currently, IPCC guidance recommends applying separate carbon burial rates to different wetland types and ecoregions to increase accuracy. However, multiple studies suggest other relevant geographic and methodological factors need to be considered in the US inventory. In some locations, accelerating sea-level rise is expanding the area conducive to carbon burial, potentially increasing carbon burial rates (Kirwan and Mudd 2012, Hill and Anisfeld 2015). A sensitivity analysis of the marsh equilibrium model highlighted



relative sea-level rise, plant productivity and relative tidal elevation as dominant drivers of carbon sequestration in stable wetlands (Morris and Callaway in Press). Elevation/inundation gradients were correlated with sediment accretion dynamics in San Francisco Bay (Callaway *et al* 2012). Finally, there are many ways to measure carbon burial that integrate different time scales: decades-  $^{137}\text{Cs}$ , centuries-  $^{210}\text{Pb}$ , or millennia-  $^{14}\text{C}$  (Turetsky *et al* 2004). We recommend that future studies rectify the complex interactions between regional variability in relative sea-level rise, plant productivity, local elevation/inundation dynamics, and the potential effects of measuring this carbon burial using differing methods.

### 3.4.2. Increasing data availability for key inputs

Some inputs in the inventory could be improved by targeted studies and additional data collection, including soil depth affected by conversion to open water, and percent carbon returned to the atmosphere upon loss.

Available data on elevation loss due to the diking of wetlands for agriculture (Drexler *et al* 2009), and the mass lost to 50 cm depth following vegetation die off (Lane *et al* 2016), are not suitable proxies for the vast majority of losses occurring from 2006 to 2011, estuarine emergent to open water conversions resulting from hurricane impacts and erosion in the Gulf of Mexico (Couvillion *et al* 2011). Although average carbon mass at depth in wetland soils is well constrained for coastal wetlands (Holmquist *et al* 2018, Sanderman *et al* 2018), the sensitivity of this carbon stock to different disturbances across regions, relative elevations, and time is not well known.

Uncertainty in assumptions about carbon loss is not unique to this study and was discussed explicitly in a recent global analysis of soil and biomass loss from mangrove conversions (Sanderman *et al* 2018), which

report that the rate and forms of carbon loss may depend on soil type and depth (Donato *et al* 2011). Because assumptions about loss events vary from study to study, and because of the fact that these assumptions are dominant contributors to uncertainty (figure 7), future research should prioritize empirical and modeling studies that constrain depth and percent carbon loss due to wetland conversion events.

### 3.4.3. Improving mapping capacity of tidal carbon relevant gradients

The wetlands supplement of the IPCC report provides two  $\text{CH}_4$  emissions factors for wetlands, one for fresh to brackish conditions and another for higher salinity (18 ppt threshold) (Poffenbarger *et al* 2011, Bridgman *et al* 2013). However, C-CAP salinity categories do not match these categories, instead mapping estuarine and palustrine (5 ppt threshold; figure 3). This inconsistency limits our ability to confidently assess the true GHG balance for saline wetlands at the national scale. We propose developing maps and data to support at least three categories of salinity—saline (>18 ppt), brackish (0.5–18 ppt), and fresh (<0.5 ppt)—in order to reduce uncertainty in landscape scale  $\text{CH}_4$  emissions from coastal wetlands (figure 4).

Existing remote sensing approaches for vegetation and inundation dynamics could improve mapping both  $\text{CH}_4$  emissions and carbon burial rates. Recent strides in mapping coastal wetland vegetation biomass (Byrd *et al* 2018), vegetation species classification (Immitzer *et al* 2016) and seasonal dynamics (Mo *et al* 2015) could provide more detailed vegetation descriptions that would be a proxy for salinity zones. For inundation/elevation regimes, extensive coastal DEMs are available, but lack the accuracy to adequately map tidal flooding depth and inundation time at relevant scales and could be improved by integrating

additional remote sensing and modeling (Hladik *et al* 2013, Parrish *et al* 2014, Buffington *et al* 2016). Future studies should quantify the precision needed for DEMs in the tidal zone. Currently soil emissions factors are calculated using tabular data, however improvements in mapping should be leveraged to support spatially-explicit approaches in future versions of the inventory incorporating trends in productivity and seasonality (Knox *et al* 2017), variation in carbon mineralization rates (Mueller *et al* 2018), edaphic factors and geomorphology (Rovai *et al* 2018). Many improvements may be forward-looking and hindcasting may not be appropriate (Byrd *et al* 2018), and spatially-explicit approaches should only be utilized only if they actually do improve precision and accuracy of inventorying compared to simpler approaches (Holmquist *et al* 2018).

Biomass changes were not a top contributor to uncertainty, but changes in forested and scrub/shrub biomass were the ninth and fifteenth contributors to uncertainty respectively. This study quantified the effect of uncertainty by upscaling means and uncertainties from multiple field studies, however remote sensing approaches using LiDAR, RADAR, object based image detection, and optical remote sensing, can all be used to characterize biomass changes on local to regional scales (Byrd *et al* 2018). Future studies could expand the uncertainty and sensitivity analysis to capture the effect that uncertainties in genus-specific assessments of wood density (Jenkins *et al* 2003), biomass carbon content (Byrd *et al* 2018), and the contributions and decay rates of downed wood (Krauss *et al* 2018).

C-CAP's accuracy was not a dominant contributor to the overall uncertainty in the inventory, but we were only able to quantify this from 2006–2011. C-CAP is available for the entire CONUS coastal zone from 1996–2011, and trends were extrapolated out back to 1990 and forward to 2015 for the NNGI inventory. Future studies are needed to assess accuracy for earlier time steps.

#### 4. Conclusions

Uncertainty in CONUS coastal wetland greenhouse gas inventory estimates comes mostly from lack of knowledge on CH<sub>4</sub> emission variability, the fate of soil carbon post-conversion, and an inability to extrapolate trends to available map products. Switching from GWP to SGW/CP increases the overall calculation of CO<sub>2e</sub> impacts from 2006–2011 by 89%. The underlying mapping products, C-CAP, and the probabilistic coastal lands layer for mapping tidal freshwater wetland extent, were not dominant contributors to uncertainty. However, the inventory development could benefit from improved change detection,

accuracy assessments that go back further in time, and improved mapping of intermediate salinities and inundation gradients. Our analysis provides a framework to track improvements to the coastal wetland GHG inventory as more data and improved process knowledge become available. The data used here were not collected for the purpose of the inventory; future improvements will demand targeted investment in data collection, model improvements, spatial product development, and more extensive, independent accuracy assessments.

#### Acknowledgments

The authors claim no conflicts of interest. Financial support was provided primarily by NASA Carbon Monitoring Systems (NNH14AY67I) and the USGS Land Carbon Program, with additional support from The Smithsonian Institution, The Coastal Carbon Research Coordination Network (DEB-1655622), and NOAA Grant: NA16NMF4630103. We would like to thank Jefferson Riera, Brian Bergamaschi, John Callaway, Judith Drexler, Rusty Feagin, Matthew Ferner, Nathan Thomas, Lisa Schile-Beers, Marc Simard, John Takekawa, and Isa Woo, David Klings, and Camille Stagg. Derivative spatial data will be made available via the Oak Ridge National Laboratory Distributed Active Archive Center (<https://doi.org/10.3334/ORNLDAAC/1650>). Code will be made available via a Smithsonian GitHub repository (<https://github.com/Smithsonian/Coastal-Wetland-NNGI-Sensitivity-Analysis>).

#### ORCID iDs

James R Holmquist  <https://orcid.org/0000-0003-2546-6766>

Lisamarie Windham-Myers  <https://orcid.org/0000-0003-0281-9581>

Blanca Bernal  <https://orcid.org/0000-0002-4879-8387>

Kristin B Byrd  <https://orcid.org/0000-0002-5725-7486>


Meagan Eagle Gonnee  <https://orcid.org/0000-0001-5072-2755>

Sara H Knox  <https://orcid.org/0000-0003-2255-5835>

Kevin D Kroeger  <https://orcid.org/0000-0002-4272-2349>

J Patrick Megonigal  <https://orcid.org/0000-0002-2018-7883>

Meng Lu  <https://orcid.org/0000-0001-6923-7493>

Ariana E Sutton-Grier  <https://orcid.org/0000-0002-1242-7728>

Donald E Weller  <https://orcid.org/0000-0002-7629-5437>

## References

- ASPRS 2004 ASPRS guidelines vertical accuracy reporting for lidar data (version 1.0) *Report for the American Society for Photogrammetry and Remote Sensing Lidar Committee (24 May)* American Society of Photogrammetry and Remote Sensing (ASPRS)
- Baldock J A, Masiello C A, Gélinas Y and Hedges J I 2004 Cycling and composition of organic matter in terrestrial and marine ecosystems *Mar. Chem.* **92** 39–64
- Barbier E B, Hacker S D and Kennedy C 2011 The value of estuarine and coastal ecosystem services *Ecological Monographs* **81** 169–93
- Blair N E and Aller R C 2012 The fate of terrestrial organic carbon in the marine environment *Ann. Rev. Mar. Sci.* **4** 401–23
- Bridgman S D, Cadillo-Quiroz H, Keller J K and Zhuang Q 2013 Methane emissions from wetlands: biogeochemical, microbial, and modeling perspectives from local to global scales *Glob. Change Biol.* **19** 1325–46
- Bridgman S D, Patrick Megonigal J, Keller J K, Bliss N B and Trettin C 2006 The carbon balance of North American wetlands *Wetlands* **26** 889–916
- Buffington K J, Dugger B D, Thorne K M and Takekawa J Y 2016 Statistical correction of lidar-derived digital elevation models with multispectral airborne imagery in tidal marshes *Remote Sens. Environ.* **186** 616–25
- Byrd K B, Ballanti L, Thomas N, Nguyen D, Holmquist J R, Simard M and Windham-Myers L 2018 A remote sensing-based model of tidal Marsh aboveground carbon stocks for the conterminous United States *ISPRS J. Photogramm. Remote Sens.* **139** 255–71
- Cai W-J 2011 Estuarine and coastal ocean carbon paradox: CO<sub>2</sub> sinks or sites of terrestrial carbon incineration? *Ann. Rev. Mar. Sci.* **3** 123–45
- Callaway J C, Borgnis E L, Eugene Turner R and Milan C S 2012 Carbon sequestration and sediment accretion in San Francisco Bay tidal wetlands *Estuaries Coasts* **35** 1163–81
- Chassereau J E, Bell J M and Torres R 2011 A comparison of GPS and lidar salt marsh DEMs *Earth Surf. Process. Landforms* **36** 1770–5
- Chmura G L, Anisfeld S C, Cahoon D R and Lynch J C 2003 Global carbon sequestration in tidal, saline wetland soils *Glob. Biogeochem. Cycles* **17** 1111
- Conrad R 1989 *Control of Methane Production in Terrestrial Ecosystems* (New York: Wiley)
- Couvillion B R *et al* 2011 *Land area change in coastal Louisiana from 1932 to 2010* Scientific Investigations Map 3164 U.S. Geological Survey
- Coveney S 2013 Association of elevation error with surface type, vegetation class and data origin in discrete-returns airborne LiDAR *Int. J. Geogr. Inf. Sci.* **27** 467–83
- DeLaune R D and White J R 2012 Will coastal wetlands continue to sequester carbon in response to an increase in global sea level?: a case study of the rapidly subsiding Mississippi river deltaic plain *Clim. Change* **110** 297–314
- Dobson J E *et al* 1995 NOAA Coastal Change Analysis Program (C-CAP): guidance for regional implementation NOAA Technical Report NMFS 123 U.S. Department of Commerce
- Donato D C, Kauffman J B, Murdiyarto D, Kurnianto S, Stidham M and Kanninen M 2011 Mangroves among the most carbon-rich forests in the tropics *Nat. Geosci.* **4** 293
- Doughty C L, Cavanaugh K C, Hall C R, Feller I C and Chapman S K 2017 Impacts of mangrove encroachment and mosquito impoundment management on coastal protection services *Hydrobiologia* **803** 105–20
- Drexler J Z, de Fontaine C S and Deverel S J 2009 The legacy of wetland drainage on the remaining peat in the Sacramento—San Joaquin Delta, California, USA *Wetlands* **29** 372–86
- EPA 2017 Land use, land-use change, and forestry *Inventory of US greenhouse gas emissions and sinks: 1990–2015*. Environmental Protection Agency EPA (<https://www.epa.gov/ghgemissions/inventory-us-greenhouse-gas-emissions-and-sinks-1990-2015>)
- Frolking S and Roulet N 2006 How northern peatlands influence the Earth's radiative budget: sustained methane emission versus sustained carbon sequestration *J. Geophys. Res.* **111** G1
- Griscom B W *et al* 2017 Natural climate solutions *Proc. Natl Acad. Sci. USA* **114** 11645–50
- Hendriks D, van Huissteden J and Dolman A J 2010 Multi-technique assessment of spatial and temporal variability of methane fluxes in a peat meadow *Agric. Forest Meteorol.* **150** 757–74
- Hill T D and Anisfeld S C 2015 Coastal wetland response to sea level rise in Connecticut and New York *Estuar. Coast. Shelf Sci.* **163** 185–93
- Hinson A L, Feagin R A, Eriksson M, Najjar R G, Herrmann M, Bianchi T S, Kemp M, Hutchings J A, Crooks S and Boutton T 2017 The spatial distribution of soil organic carbon in tidal wetland soils of the continental United States *Glob. Change Biol.* **23** 5468–80
- Hladik C, Schalles J and Alber M 2013 Salt Marsh elevation and habitat mapping using hyperspectral and LIDAR data *Remote Sens. Environ.* **139** 318–30
- Holmquist J R *et al* 2018 Accuracy and precision of tidal wetland soil carbon mapping in the conterminous United States *Sci. Rep.* **8** 9478
- Howard J, Sutton-Grier A, Herr D, Kleypas J, Landis E, Mcleod E, Pidgeon E and Simpson S 2017 Clarifying the role of coastal and marine systems in climate mitigation *Front. Ecol. Environ.* **15** 42–50
- Immitzer M, Vuolo F and Atzberger C 2016 First experience with sentinel-2 data for crop and tree species classifications in central Europe *Remote Sensing* **8** 166
- IPCC 1997 *Greenhouse Gas Inventory: Revised 1996 IPCC Guidelines for National Greenhouse Gas Inventories* ed J T Houghton (Bracknell: IPCC)
- IPCC 2006 *IPCC Guidelines for National Greenhouse Gas Inventories, Prepared by the National Greenhouse Gas Inventories Programme* ed H S Eggleston, L Buendia, K Miwa, T Ngara and K Tanabe (Kanagawa Prefecture: IGES)
- IPCC 2014 *2013 Supplement to the 2006 IPCC Guidelines for National Greenhouse Gas Inventories: Wetlands* ed T Hiraishi (Bracknell: IPCC)
- Jenkins J C, Chojnacky D C, Heath L S and Birdsey R A 2003 National-scale biomass estimators for United States tree species *For. Sci.* **49** 12–35
- Kirwan M L and Megonigal J P 2013 Tidal wetland stability in the face of human impacts and sea-level rise *Nature* **504** 53–60
- Kirwan M L and Mudd S M 2012 Response of salt-marsh carbon accumulation to climate change *Nature* **489** 550–3
- Kirwan M L, Temmerman S, Skeehean E E, Guntenspergen G R and Fagherazzi S 2016 Overestimation of marsh vulnerability to sea level rise *Nat. Clim. Chang.* **6** 253–60
- Knox S H, Dronova I, Sturtevant C, Oikawa P Y, Matthes J H, Verfaillie J and Baldocchi D 2017 Using digital camera and Landsat imagery with eddy covariance data to model gross primary production in restored wetlands *Agric. Forest Meteorol.* **237–238** 233–45
- Krauss K W, Demopoulos A W J, Cormier N, From A S, McClain-Counts J P and Lewis R R 2018 Ghost forests of Marco Island: mangrove mortality driven by belowground soil structural shifts during tidal hydrologic alteration *Estuar. Coast. Shelf Sci.* **212** 51–62
- Krauss K W, Holm G O, Perez B C, McWhorter D E, Cormier N, Moss R F, Johnson D J, Neubauer S C and Raynie R C 2016 Component greenhouse gas fluxes and radiative balance from two deltaic Marshes in Louisiana: pairing chamber techniques and eddy covariance *J. Geophys. Res. Biogeosci.* **121** 2015JG003224
- Kroeger K D, Crooks S, Moseman-Valtierra S and Tang J 2017 Restoring tides to reduce methane emissions in impounded wetlands: a new and potent blue carbon climate change intervention *Sci. Rep.* **7** 11914
- Lane R R, Mack S K, Day J W, DeLaune R D, Madison M J and Precht P R 2016 Fate of soil organic carbon during wetland loss *Wetlands* **36** 1167–81

- Leon J X, Heuvelink G B M and Phinn S R 2014 Incorporating DEM uncertainty in coastal inundation mapping *PLoS One* **9** e108727
- Levy P E, Cowan N, van Oijen M, Famulari D, Drewer J and Skiba U 2017 Estimation of cumulative fluxes of nitrous oxide: uncertainty in temporal upscaling and emission factors *Eur. J. Soil Sci.* **68** 400–11
- Lovelock C, Fourqurean J and Morris J 2017 Modeled CO<sub>2</sub> emissions from coastal wetland transitions to other land uses: tidal Marshes, mangrove forests and seagrass beds *Frontiers Mar. Sci.* **4** 143
- McCombs J W, Herold N D, Burkhalter S G and Robinson C J 2016 Accuracy assessment of NOAA coastal change analysis program 2006–2010 land cover and land cover change data *Photogramm. Eng. Remote Sens.* **82** 711–8
- Metsaranta J M, Shaw C H, Kurz W A, Boisvenue C and Morken S 2017 Uncertainty of inventory-based estimates of the carbon dynamics of Canada's managed forest (1990–2014) *Can. J. For. Res.* **47** 1082–94
- Morris J T and Callaway J C 2019 Physical and biological regulation of carbon sequestration in tidal marshes *A Blue Carbon Primer: The State of Coastal Wetland Carbon Science, Practice and Policy* ed L Windham-Meyers *et al* (London: Taylor and Francis) pp 498
- Morris J T, Sundareshwar P V, Nietch C T, Kjerfve B and Cahoon D R 2002 Responses of coastal wetlands to rising sea level *Ecology* **83** 2869–77
- Mo Y, Momen B and Kearney M S 2015 Quantifying moderate resolution remote sensing phenology of Louisiana coastal marshes *Ecol. Modell.* **312** 191–9
- Mueller P *et al* 2018 Global-change effects on early-stage decomposition processes in tidal wetlands—implications from a global survey using standardized litter *Biogeosciences* **15** 3189–202
- Najjar R G *et al* 2018 Carbon budget of tidal wetlands, estuaries, and shelf waters of Eastern North America *Glob. Biogeochem. Cycles* **32** 389–416
- Neubauer S C and Megonigal J P 2015 Moving beyond global warming potentials to quantify the climatic role of ecosystems *Ecosystems* **18** 1000–13
- Nyman J A, Walters R J, Delaune R D and Patrick W H 2006 Marsh vertical accretion via vegetative growth *Estuar. Coast. Shelf Sci.* **69** 370–80
- Ogle S M, Jay Breidt F, Eve M D and Paustian K 2003 Uncertainty in estimating land use and management impacts on soil organic carbon storage for US agricultural lands between 1982 and 1997 *Glob. Change Biol.* **9** 1521–42
- Olofsson P, Foody G M, Herold M, Stehman S V, Woodcock C E and Wulder M A 2014 Good practices for estimating area and assessing accuracy of land change *Remote Sens. Environ.* **148** 42–57
- Ouyang X and Lee S Y 2013 Carbon accumulation rates in salt marsh sediments suggest high carbon storage capacity *Biogeosci. Discuss.* **10** 19155–88
- Pachauri R K *et al* 2014 *Climate Change 2014: Synthesis Report. Contribution of Working Groups I, II and III to the Fifth Assessment Report of the Intergovernmental Panel on Climate Change* ed R K Pachauri and L Meyer (Bracknell: IPCC)
- Parrish C E, Rogers J N and Calder B R 2014 Assessment of waveform features for lidar uncertainty modeling in a coastal salt marsh environment *IEEE Geosci. Remote Sens. Lett.* **11** 569–73
- Pendleton L *et al* 2012 Estimating global 'blue carbon' emissions from conversion and degradation of vegetated coastal ecosystems *PLoS One* **7** e43542
- Poffenbarger H J, Needelman B A and Patrick Megonigal J 2011 Salinity influence on methane emissions from tidal marshes *Wetlands* **31** 831–42
- Rovai A S, Twilley R R, Castañeda-Moya E, Riul P, Cifuentes-Jara M, Manrow-Villalobos M, Horta P A, Simonassi J C, Fonseca A L and Pagliosa P R 2018 Global controls on carbon storage in mangrove soils *Nat. Clim. Change* **8** 534–8
- Sanderman J *et al* 2018 A global map of mangrove forest soil carbon at 30 m spatial resolution *Environ. Res. Lett.* **13** 055002
- Schmid K, Hadley B and Waters K 2013 Mapping and portraying inundation uncertainty of bathtub-type models *J. Coast. Res.* **30** 548–61
- Stein E D, Cayce K, Salomon M, Bram D L, De Mello D, Grossinger R and Dark S 2014 Wetlands of the Southern California coast: historical extent and change over time *Southern California Coastal Water Research Project Technical Report Technical Report 826 and SFEI Report 720* Southern California Coastal Water Research Project and San Francisco Estuary Institute ([http://sfei.org/sites/default/files/826\\_Coastal%20Wetlands%20and%20change%20over%20time\\_Aug%202014.pdf](http://sfei.org/sites/default/files/826_Coastal%20Wetlands%20and%20change%20over%20time_Aug%202014.pdf))
- Turetsky M R, Manning S W and Wieder R K 2004 Dating recent peat deposits *Wetlands* **24** 324–56
- Walter B P and Heimann M 2000 A process-based, climate-sensitive model to derive methane emissions from natural wetlands: application to five wetland sites, sensitivity to model parameters, and climate *Glob. Biogeochem. Cycles* **14** 745–65
- Wang Z, Zeng D and Patrick W H Jr 1996 Methane emissions from natural wetlands *Environ. Monit. Assess.* **42** 143–61
- Weston N B, Neubauer S C, Velinsky D J and Vile M A 2014 Net ecosystem carbon exchange and the greenhouse gas balance of tidal marshes along an estuarine salinity gradient *Biogeochemistry* **120** 163–89
- Whalen S C 2005 Biogeochemistry of methane exchange between natural wetlands and the atmosphere *Environ. Eng. Sci.* **22** 73–94
- Windham-Myers L *et al* 2018 Tidal wetlands and estuaries *Second State of the Carbon Cycle Report (SOCCR2): A Sustained Assessment Report* ed N Cavallaro, G Shrestha, R Birdsey, M A Mayes, R Najjar, S Reed, P Romero-Lankao and Z Zhu (Washington, DC: U.S. Global Change Research Program)
- Wylie L, Sutton-Grier A E and Moore A 2016 Keys to successful blue carbon projects: lessons learned from global case studies *Mar. Policy* **65** 76–84